

Article

3D Printing-Assisted versus Conventional Extracorporeal Fenestration Tevar for Stanford Type B Arteries Dissection with Undesirable Proximal Anchoring Zone: Efficacy Analysis

Rongyi Zheng¹, Fangtao Zhu¹, Cunwei Cheng¹, Weihua Huang¹,
Haojie Zhang¹, Xin He¹, Qianqian Lu¹, Huayuan Xi², Kailin Shen¹, Haibin Yu^{1,*}

¹The Second Affiliated Hospital of Zhengzhou University, 450000 Zhengzhou, Henan, China

²The Fifth Affiliated Hospital of Zhengzhou University, 450000 Zhengzhou, Henan, China

*Correspondence: 1624775141@qq.com (Haibin Yu)

Submitted: 27 June 2023 Revised: 31 July 2023 Accepted: 7 August 2023 Published: 23 August 2023

Abstract

Background: To compare the outcomes of two Thoracic Endovascular Aortic Repair (TEVAR) techniques of Left Subclavian Artery (LSA) reconstruction for Stanford Type B Aortic Dissection (TBAD) patients with undesirable proximal anchoring zone. **Methods:** We retrospectively reviewed 57 patients with TBAD who underwent either three dimensional (3D)-printing-assisted extracorporeal fenestration (n = 32) or conventional extracorporeal fenestration (n = 25) from December 2021 to January 2023. We compared their demographic characteristics, operative time, technical success rate, complication rate, secondary intervention rate, mortality rate, and aortic remodeling. **Results:** Compared with the conventional group, the 3D-printing-assisted group had a significantly shorter operative time (147.84 ± 33.94 min vs. 223.40 ± 65.93 min, $p < 0.001$), a significantly lower rate of immediate endoleak (3.1% vs. 24%, $p = 0.048$) and a significantly higher rate of true lumen diameter expansion in the stent-graft segment (all $p < 0.05$), but a significantly longer stent graft modification time (37.63 ± 2.99 min vs. 28.4 ± 2.12 min, $p < 0.001$). There were no significant differences in other outcomes between the two groups ($p > 0.05$). The degree of false lumen thrombosis was higher in the stent-graft segment than in the non-stent-graft segment in both groups and the difference was statistically significant ($X^2 = 5.390, 4.878$; $p = 0.02, 0.027$). **Conclusions:** Both techniques are safe and effective for TBAD with an undesirable proximal landing zone. The 3D-printing-assisted extracorporeal fenestration TEVAR technique has advantages in operative time, endoleak risk, and aortic remodeling, while the traditional extracorporeal fenestration TEVAR technique has advantages in stent modification.

Keywords

stanford type B aortic dissection; 3D printing; extracorporeal fenestration TEVAR; undesirable proximal anchoring zone

Introduction

Thoracic endovascular aortic repair (TEVAR) is a preferred treatment option for Stanford type B aortic dissection (TBAD) patients because it is less invasive and has fewer adverse effects [1,2]. However, TEVAR requires a proximal landing zone of at least 15 mm [3], and an undesirable proximal landing zone may compromise the success of TEVAR [4]. Therefore, TBAD patients with an insufficient proximal landing zone often need to cover the left subclavian artery (LSA) to obtain adequate anchoring, but this may cause serious complications, such as cerebral ischemia, LSA steal syndrome, spinal cord ischemia, and even death [5]. To reduce postoperative complications as much as possible, LSA revascularization has become a consensus among more and more experts and scholars [6]. With the increasing maturity of three-dimensional (3D) printing technology, its unique advantages in simulating complex aortic anatomy and morphology are more obvious [7]. 3D-printing-assisted extracorporeal fenestration TEVAR involves using 3D printing technology to create a model of the patient's aorta, and according to the position and diameter of LSA on the model, precisely fenestrate the stent graft *ex vivo*, and then place the fenestrated stent graft in the patient's aorta to achieve the accurate reconstruction of LSA [8,9]. This technique can overcome the limitations of conventional extracorporeal fenestration TEVAR, such as inaccurate fenestration position, inappropriate fenestration diameter, damage to stent graft during fenestration, etc. In addition, combined with cinching technique, the stent graft can be positioned and adjusted multiple times in the vessel, which further improves the success rate of surgery. However, the specific advantages and disadvantages of the two techniques in treating TBAD patients with an insufficient proximal landing zone need to be further studied. A comparative study of clinical efficacy in the same center and an assessment of short-term and mid-term clinical outcomes are still lacking [10]. Hence, this study aims to evaluate the short-term and mid-term clinical outcomes, strengths and weaknesses of 3D printing-assisted extracor-

Table 1. Preoperative detailed data and complications of patients.

Clinical data	3D printing-assisted extracorporeal pre-windowing group (n = 32)	Traditional extracorporeal windowing group (n = 25)	X ²	p
Male	22	17	0.004	0.952
Hypertension	24	19	0.008	0.931
Cardiac insufficiency	13	7	0.982	0.322
Coronary atherosclerotic heart disease	11	8	0.036	0.850
Renal insufficiency	6	3	0.107	0.743
Diabetes mellitus	9	8	0.101	0.751

poreal fenestration TEVAR versus conventional extracorporeal fenestration TEVAR for treating TBAD patients with undesirable proximal anchoring zone.

Materials and Methods

General Data

This study employed a retrospective analysis method to collect the clinical data of 57 patients with TBAD affecting LSA who received TEVAR treatment at our center from December 2021 to January 2023. The patients were categorized into two groups based on the different surgical methods: the 3D printing-assisted extracorporeal pre-windowing group (n = 32) and the traditional extracorporeal pre-windowing group (n = 25). All patients underwent aortic computed tomography angiography (CTA) before surgery to identify aortic dissection (AD), and the proximal landing zone was <15 mm. They were classified according to their type following the guideline [1], with 15 cases in hyperacute (<24 hours) and 42 cases in acute (1–14 days). The high-risk factors of the patients are presented in Table 1, which met the criteria for TEVAR surgery. The inclusion criteria were: (1) Diagnosed as type B AD based on the patient's medical history and preoperative CTA, according to the AD classification criteria (Stanford classification); (2) Preoperative CTA indicated that the distance between the intimal tear and LSA was <15 mm; (3) Preoperative CTA demonstrated that the dissection retrograde tear or hematoma had involved LSA; (4) No severe liver or kidney dysfunction. Exclusion criteria: (1) Type A aortic dissection, dissection retrograde tear or hematoma involving ascending aorta, *etc.*; (2) Patients who only underwent single branch artery reconstruction of LSA during surgery; (3) Patients who did not apply extracorporeal pre-windowing TEVAR technique; (4) Patients with hereditary connective tissue disease (such as Marfan syndrome). This study was approved by the Ethics Committee of Zhengzhou University Second Affiliated Hospital (Approval No: 2023167) and all patients signed informed consent before surgery.

Preoperative Data Collection and 3D Printing Model Fabrication

The patient's original CTA Digital Imaging and Communications in Medicine (DICOM) data were entered into Endosize software (Therenva SAS corp, Bretagne, France), and 3D image reconstruction was conducted to measure the following key points of the aorta: the aortic lesion (aortic aneurysm or true and false lumen of dissection), the planned proximal and distal landing zones and the inner diameter and lesion length of significant branch arteries. After verifying that the patient satisfied the condition, lesion scope and anatomical criteria for fenestrated/branched thoracic endovascular aortic repair (F/B-TEVAR), a surgical strategy was devised. Firstly, the original data file was entered into Mimics 21.0 software (Materialise corp, Louvain, Belgium), and 3D reconstruction of the aortic arch region (including the proximal and distal normal aorta, affected aorta and vital branch openings of the arch) was carried out. Then, the reconstructed 3D model data were entered into the design software (Geomagic Studio 2014, Geomagic corp, Triangle Development Zone, North Carolina, USA) for further preprocessing. Using reverse engineering technology, non-parametric surface reconstruction was applied to the blood vessels to obtain the computer-aided design (CAD) mathematical model of the blood vessels (see Fig. 1A). Using design software (Geomagic Studio 2014, Geomagic corp, Triangle Development Zone, North Carolina, USA), simulation analysis was executed. Based on the surgical strategy, the window positioning holes of the main branch arteries of the aortic arch were identified, and a 3D printing guide plate was designed (see Fig. 1B). Finally, the guide plate was sent to Stratasys Eden260VS 3D printer (Stratasys company, Eden Prairie, Minnesota, USA), and a hollow 3D aortic model close to the patient's affected aorta was fabricated with imported photosensitive resin as raw material. Each model cost \$410, and finally, the printed 3D aortic model (see Fig. 2A) was sterilized and sealed with ethylene oxide.

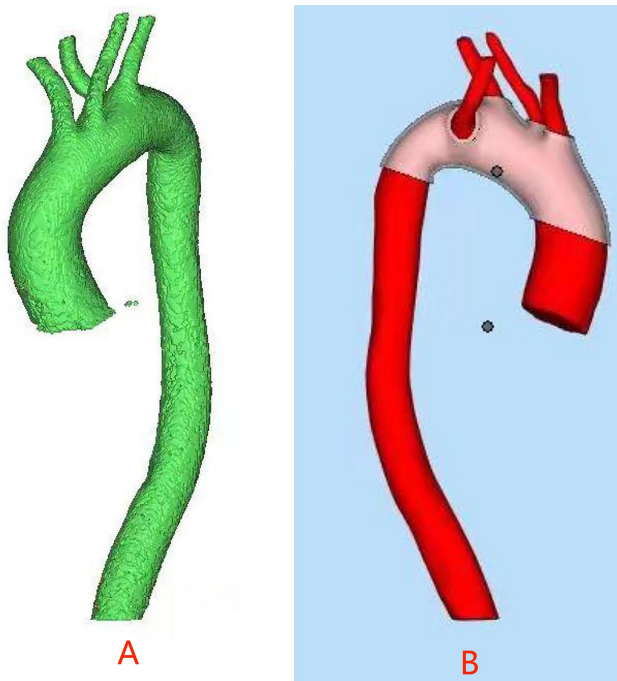


Fig. 1. Three-dimensional (3D) printing process. (A) 3D aortic simulation model. (B) Design of 3D printing window guide plate.

Operation Methods

Stent Modification

The diameter of the main stent was generally chosen to be about 10% larger than the CTA measurement value, and an appropriate size of Ankura (Xianjian) covered stent main body was deployed in the sterilized 3D printed model to determine the window location and diameter (see Fig. 2A). An electrode pen was used to rupture the membrane, and suturing of the stent lining, extension support, *etc.* It was selected at the window to decrease the occurrence of endoleak (see Fig. 2B). The V18 guidewire was passed through the 6 o'clock direction of the main stent (with the arch vertex as the 12 o'clock position), and a hole was made on the delivery sheath, and one end of the guidewire was drawn out from here. The main stent was reduced (at least 30%~45%) with 5-0 Prolene thread (Johnson, New Brunswick, New Jersey, USA) and secured on the guidewire to complete the bundle diameter and then retracted into the delivery system (see Fig. 2C), and then the stent delivery system was pre-bent in the sterilized 3D printed model stent to make it more conformable to the curvature of the aortic arch, facilitating successful deployment (see Fig. 2D). The conventional extracorporeal windowing group determined the window location and diameter on the main stent (Medtronic Minneapolis, Minnesota, USA) (Xinmai, Shanghai, China) based on the patient's aortic CTA data and the surgeon's experience, and used an electrode pen to rupture the membrane. The window location marker (Marker used a spring ring, which was sewn around the window edge with 5-0

Prolene), and finally retracted the stent into the delivery system.

Delivery and Deployment of the Stent

A direct incision was made in the left groin, a segment of femoral artery was mobilized for standby, punctured left femoral artery, placed 6F femoral sheath, administered 5000 u heparin anticoagulation treatment. Guided by a super-slip guidewire, a pigtail catheter was advanced to the ascending aorta plane, a high-pressure syringe angiography confirmed that the catheter was in the true lumen of dissection, exchanged for a super-hard guidewire to reach the bottom of aortic sinus. Withdraw femoral sheath, deliver main stent delivery system via super-hard guidewire, partially deploy stent when main stent reaches aortic arch to expose window hole, reduce front end diameter of main stent by 30%~45% under bundle diameter state, can fine-tune to facilitate "super-selection" through branch artery for window hole. Puncture left brachial artery, place 6F radial sheath, administered 5000 u heparin anticoagulation treatment. Guidewire catheter cooperation under super-selection to stent pre-window hole, make stent window location correspond to branch vessel. Control blood pressure, deploy main stent, complete window hole "super-selection" after entering long sheath via brachial artery route, introduce branch stent and deploy, withdraw V-18 bundle diameter guidewire, fully deploy main stent. Intraoperative angiography again confirmed whether there was endoleak and stent stenosis occlusion, whether branch vessel blood flow was smooth. Postoperative dual anti-treatment for 3 months for patients, according to patient condition continue dual anti or change to single anti-treatment.

Follow-Up and Evaluation Methods

Postoperative follow-up was conducted through multiple channels such as ward rounds, telephone inquiries, outpatient visits, *etc.* (7~30 days, six months, and one year after surgery). The clinical outcomes measures included operative success rate, device deployment success rate (defined as successful positioning and release of the main stent graft during surgery, successful isolation of aneurysm, dissection proximal tear, *etc.*), intraoperative and postoperative complication rate, secondary intervention rate, mortality rate, *etc.* Patients underwent regular CTA examination to assess the patency of the main stent graft and fenestration stent graft and the occurrence of endoleak. Four aortic planes were selected for measurement (as shown in the Fig. 3), and the maximum diameter perpendicular to the intimal flap was measured in each plane. The changes in true and false lumen diameters in different aortic planes before and after surgery and the degree of thrombosis in the false lumen after surgery were compared to evaluate aortic remodeling.

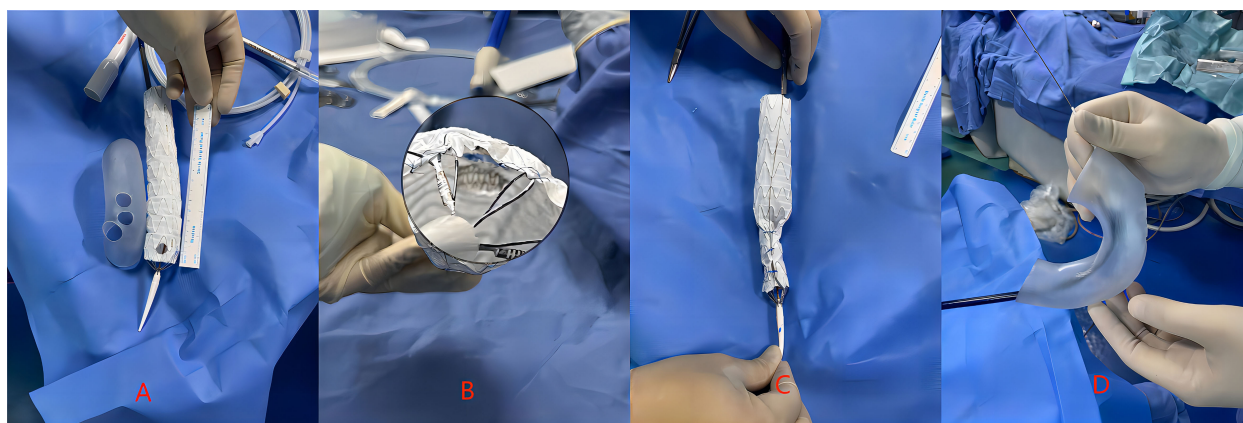


Fig. 2. 3D printed aortic model to guide stent modification. (A) 3D printing model of the aortic arch and windowing of main stent according to 3D model. (B) Sewn embedded branch stent in main stent. (C) Treatment of main stent bundle diameter. (D) Pre-bending treatment of main stent in 3D printing model.

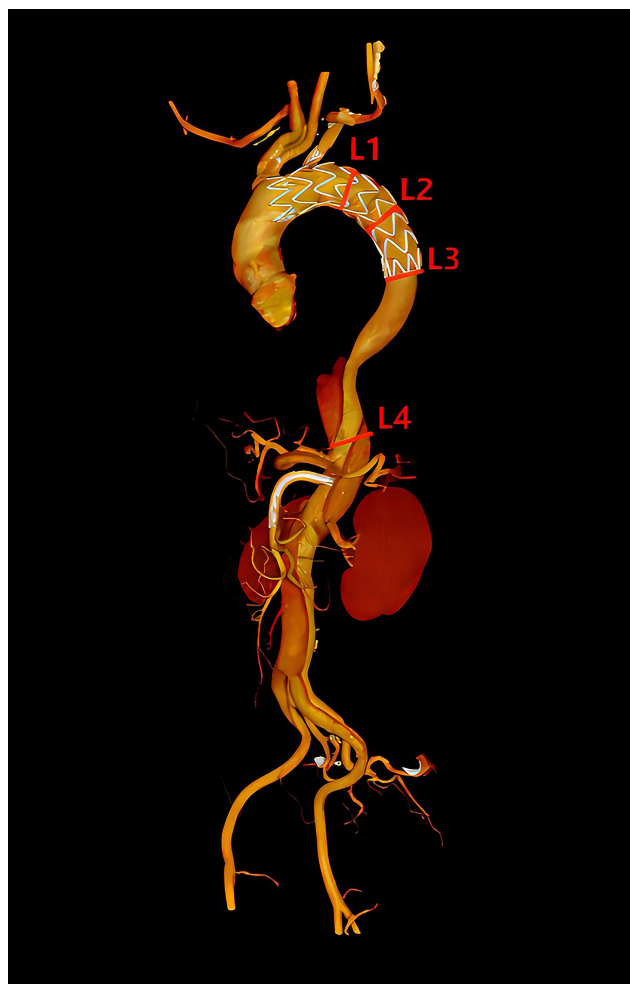


Fig. 3. Measuring plane. L1, the aortic plane about 1cm distal to the root of LSA; L2, the aortic plane at the lower edge of the tracheal bifurcation; L3, the plane of the distal anchoring area of the stent; L4, the aortic plane at the level of the aortic hiatus (about the 12 th thoracic body). LSA, Left Subclavian Artery.

Statistical Analysis

SPSS 27.0 software (IBM Corp., Armonk, NY, USA) was used for the statistical analysis of data. Data with normal distribution were analyzed by independent samples *t*-test, and data with non-normal distribution were analyzed by non-parametric test (Mann-Whitney U test). Categorical data were compared by chi-square test or Fisher exact test. Two-sided test, significance level $\alpha = 0.05$.

Results

Patient Clinical Data

There was no significant difference in age ($x \pm s$) between the two groups (55.14 ± 11.14 vs. 56.16 ± 13.02 , $t = 0.235$, $p = 0.815 > 0.05$). The preoperative data and complications of the patients are presented in Table 1. The basic data did not differ significantly between the two groups ($p > 0.05$).

Perioperative Complications Results of Both Groups of Patients

The 3D-printing-assisted group had a significantly shorter operative time than the conventional group (147.84 ± 33.94 min vs. 223.40 ± 65.93 min, $p < 0.001$), but a significantly longer stent graft modification time than the conventional group (37.63 ± 2.99 min vs. 28.4 ± 2.12 min, $t = 13.054$, $p < 0.001$). The device deployment success rate was 100% in both groups, with no significant difference ($p > 0.05$). The 3D-printing-assisted group also had a significantly lower rate of postoperative endoleak than the conventional group (3.1% vs. 24%, $p = 0.048$), while there were no significant differences in other complication rates, secondary intervention rates and mortality rates between the two groups ($p > 0.05$). The perioperative complications

Table 2. Results of perioperative period and complications.

Clinical data	3D printing-assisted extracorporeal pre-windowing group (n = 32)	Traditional external windowing group (n = 25)	X ²	p
Operation infection	3	5	0.580	0.446
Postoperative cerebral infarction	1	3	0.607	0.436
Post-operational pain	2	4	0.571	0.450
Postoperative limb weakness	0	1		0.439
Internal leakage	1	6	3.905	0.048

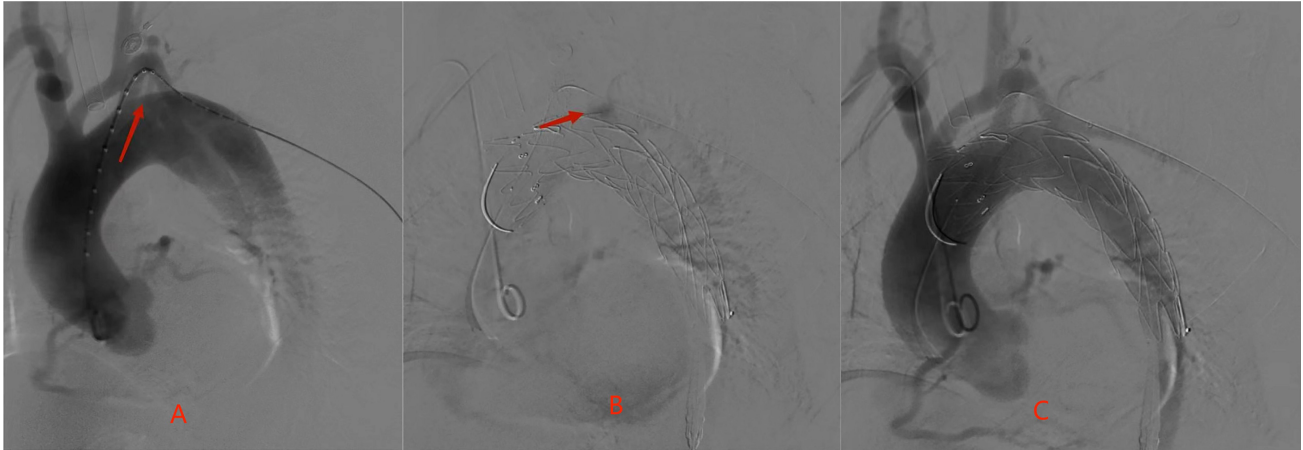


Fig. 4. Intraoperative angiography pictures. (A) Angiography prompted dissection rupture adjacent to the left subclavian artery (red arrows). (B) Angiography, after stent release visible contrast agent leakage (red arrows) consider for stent fenestration diameter, is too large to cause stent junction leakage. (C) Balloon dilatation after angiography prompted leakage disappeared.

results are shown in Table 2. Among them, one case of type II endoleak occurred in the 3D-printing-assisted group, which was not treated and resolved after one month of angiographic follow-up. Four cases of type I endoleak occurred in the conventional group (see Fig. 4), which were attributed to too large fenestration diameter, poor alignment of fenestration position and LSA ostium, and were managed by balloon dilation, filling coils (cook) in the gap and angiography again. Two cases of type II endoleak occurred in the conventional group, which were not treated and resolved after one month of angiographic follow-up.

Follow-Up Results

The follow-up time of the two groups was (16.14 ± 3.76) and (7.97 ± 3.80) months ($t = 8.086$, $p < 0.001$). The significant difference in follow-up time was due to the later application of 3D printing-assisted TEVAR with extracorporeal fenestration technique than conventional TEVAR with extracorporeal fenestration technique in our center. During the follow-up period, there were no new endoleaks and complications such as spinal cord and limb ischemia in both groups, one case of new dissection at the distal end of the stent in the conventional group, and one patient who died of Corona Virus Disease 2019 (COVID-19) seven months after surgery. There was no significant difference in survival rate between the two groups ($p = 0.439 > 0.05$).

Comparison of Aortic Remodeling after Dissection between the Two Groups

The preoperative and postoperative one-month thoracic and abdominal aortic CTA data of the two groups of patients were collected, and three-dimensional reconstruction and measurement were performed using Endosize. The results are shown in Table 3. In the stent-graft segment (L1, L2, and L3 planes), the 3D-printing-assisted group had a higher rate of true lumen diameter expansion than the conventional group (all $p < 0.05$), while there was no significant difference in the changes in true and false lumen diameters between the two groups in the non-stent-graft segment (L4 plane) (all $p > 0.05$). There was no statistically significant difference in thrombosis between the stent and non-stent segments between the two groups (all $p > 0.05$). The results are shown in Table 4. While the degree of false lumen thrombosis was higher in the stent-graft segment than in the non-stent-graft segment in both groups and the difference was statistically significant ($X^2 = 5.390, 4.878$; $p = 0.02, 0.027$).

Discussion

3D printing technology has a broad application and excellent effect in mimicking aortic morphology, but most

Table 3. The changes in true and false lumen diameters in different aortic planes between two groups.

Plane	Rate of change	3D printing-assisted extracorporeal pre-windowing group (n = 32)	Traditional extracorporeal pre-windowing group (n = 25)	<i>p</i>
L1	R (DTL)	56.66 ± 31.02	31.87 ± 16.94	<0.001
	R (DFL)	-85.25 ± 24.30	-91.22 ± 9.50	0.008
L2	R (DTL)	72.55 ± 41.42	41.75 ± 21.78	<0.001
	R (DFL)	-85.95 ± 27.52	-85.05 ± 27.20	0.878
L3	R (DTL)	72.40 ± 36.65	50.51 ± 37.05	0.004
	R (DFL)	-84.15 ± 24.53	-79.59 ± 29.47	0.345
L4	R (DTL)	40.64 ± 55.42	27.67 ± 22.29	0.563
	R (DFL)	-36.54 ± 37.13	-22.11 ± 28.48	0.125

Note: R (DTL) is the rate of true lumen diameter expansion, R (DFL) is the rate of false lumen diameter expansion, rate of true and false lumen area or diameter expansion = (postoperative true and false lumen diameter – preoperative true and false lumen diameter) / preoperative true and false lumen diameter × 100%.

Table 4. The degree of thrombosis in the false lumen of thrombus in the two groups.

Site	Degree of false lumen thrombosis	3D printing-assisted extracorporeal pre-windowing group (n = 32)	Traditional extracorporeal pre-windowing group (n = 25)	X ²	<i>p</i>
Aortic stent segment	Complete thrombosis or disappearance of false lumen	25	19	0.450	0.888
	Partial thrombosis	5	5		
	No thrombosis	2	1		
Aortic non-stent segment	Complete thrombosis or disappearance of false lumen	7	6	0.205	0.942
	Partial thrombosis	16	11		
	No thrombosis	9	8		

studies only focus on its role in mimicking aortic anatomical structure [11,12], and lack research on its role in treating TBAD patients with inadequate proximal landing zone [13]. This study innovatively employed 3D printing technology to assist the extracorporeal LSA pre-windowing technique, offering a new individualized treatment option for TBAD patients with unfavorable proximal landing zone, using preoperative and postoperative four-plane true and false lumen change rate, stent thrombosis rate, patient survival rate and complication incidence rate to assess the efficacy and clinical outcomes of this surgical method, and compared it with the conventional extracorporeal windowing technique in detail, aiming to more realistically and specifically evaluate the benefits and suitability of 3D printing-assisted extracorporeal pre-windowing technique.

This study compared and analyzed the short- and medium-term clinical outcomes of 3D printing-assisted extracorporeal pre-windowing technique and conventional extracorporeal pre-windowing technique in treating TBAD patients with undesirable proximal anchoring zone, both of which have good safety and efficacy, which is in line with domestic and international research results [14, 15]. However, the 3D printing-assisted extracorporeal pre-windowing technique has evident advantages over conventional extracorporeal pre-windowing technique, mainly manifested in the following aspects: First, in terms of

surgery time, the 3D printing-assisted extracorporeal pre-windowing group surgery time (147.84 ± 33.94) was significantly shorter than traditional extracorporeal pre-windowing group (223.40 ± 65.93) (*p* < 0.001), which may be related to the following reasons: (1) 3D printing technology can create a dissection model that conforms to the patient's aortic anatomical morphology in advance, and achieve precise extracorporeal windowing based on this model, thus providing more intuitive, more accurate, and safer guidance for the surgery [16]; (2) Combined with bundle diameter technology, the main stent diameter is reduced by at least 30%–45% and retracted into the delivery system, which can achieve a larger range of adjustment in the vascular cavity, making it easier for the branch artery guidewire to super-select into the window, shortening the alignment time and release time of the stent window position and branch artery, thereby shortening the surgery time [17,18]; (3) Reduced the possibility of stent modification or secondary surgical intervention due to inaccurate window position or unsuitable window diameter. Second, in terms of postoperative complications, the 3D printing-assisted extracorporeal pre-windowing group's immediate angiography endoleak situation after stent deployment was also significantly lower than simple extracorporeal windowing group (*p* < 0.05), which may be related to the following reasons: This may be related to 3D printing technology can enhance

the fit between the stent and the aortic wall and arch branch arteries. Through a 3D printing model, we can suture an embedded stent at the window to form a seamless connection between it and the left subclavian artery [19,20]. Postoperative false lumen reduction and thrombosis are reliable indicators for evaluating the long-term prognosis of TBAD patients [21,22]. The 3D printing-assisted extracorporeal pre-windowing group's true lumen diameter dilation rate was significantly higher than conventional extracorporeal windowing group ($p < 0.05$), which may be related to simulating stent deployment in the patient's 3D aortic model before surgery, determining appropriate deployment angle and position to make the stent main body fit well with aortic wall, effectively sealing dissection tear and channel, reducing false lumen diameter, and promoting false lumen thrombosis. In both groups, the postoperative stent segment false lumen thrombosis degree was significantly better than the non-stent segment, the difference was significant ($p < 0.05$), and the stent segment dissection aorta remodeling effect was better [23,24].

3D printing technology can accurately produce complex anatomical models of pathologies, providing a powerful auxiliary tool for surgeons to facilitate disease diagnosis, decision making and treatment planning [25]. In recent years, this technology has been widely used in the treatment of thoracic aortic dissection (TBAD) with an insufficient proximal landing zone by fenestration creation of aortic stent grafts *in vitro* and has achieved good results. 3D printed aortic models have two advantages in the modification of aortic stent grafts: (1) 3D printed models are hollow and transparent, which can allow accurate fenestration positioning of the aortic stent grafts after opening in the 3D printed models, avoiding errors caused by manual measurement; (2) The precise replication of the aortic arch can simulate the position of the aortic stent graft after implantation *in vivo*, and the position of the branch vessel orifice is more accurate than simply measuring from CTA, thus accurately simulating the spatial relationship between the aortic stent graft and the arch branches. For aortic anatomical variations such as bovine aortic arch, aberrant right subclavian artery, left vertebral artery originating from the aortic arch, *etc.*, and severe tortuosity or angulation of the aortic arch such as type III aortic arch, the complex anatomical conditions of the patient's aortic arch make it difficult for the stent graft fenestration to match the branch vessel orifice, increasing the difficulty of surgery, reducing the success rate of surgery, and prolonging the operation time. Using 3D printing technology to produce these anatomically complex aortic arch models can not only visually demonstrate the anatomical structure of the pathology, but also simulate the distortion of the intraluminal stent graft, thus enabling more accurate fenestration design, reducing the difficulty of surgery and ensuring the safety of surgery [26]. In addition to guiding physicians in the fenestration creation of aortic stent grafts, 3D printed models can also clearly show the

morphology and anatomical relationship of the aorta and its branches, facilitating doctors and patients to understand the disease and surgical plan, enhancing doctor-patient communication, and improving the education of young doctors on aortic diseases [27].

Limitations

Although 3D printing-assisted aortic stent windowing has higher precision than manual measurement of stent windowing, the stress interaction between the 3D printed model and the aortic stent differs from the actual aorta. Due to the existence of multiple twisted angles from the femoral artery to the thoracic aorta, when the main stent is introduced to the aortic arch, the vessel may be twisted by the stress of the super-hard guidewire and the stiff stent delivery device, resulting in displacement between the stent window and the arch vessel opening [28]. The current 3D-printing aortic model material is hard and cannot fully mimic the changes of the aorta after stress [29]. With the further advancement of 3D printing technology, we anticipate materials with flexibility and elasticity closer to the aorta to emerge, to more ideally mimic the real condition of the aortic arch, while minimizing the preparation time of the model as much as possible, so that patients with critical conditions who require emergency surgery can also benefit. Of course, we also acknowledge that there are some limitations in this study, such as small sample size, short follow-up time, medium- and long-term treatment outcomes that still need further follow-up and assessment, *etc.* Therefore, we need to conduct larger-scale, longer-term, more rigorous randomized controlled trials to validate the superiority and feasibility of the 3D printing-assisted extracorporeal pre-windowing technique in treating TBAD patients with inadequate proximal landing zone.

Conclusions

From the above case data, both techniques have good safety and efficacy in treating Stanford type B aortic dissection with inadequate proximal landing zone. The 3D printing-assisted extracorporeal pre-fenestration technique has more benefits in shortening operative time, lowering endoleak risk, enhancing true lumen diameter expansion rate, facilitating aortic remodeling, *etc.* While conventional extracorporeal fenestration technique has advantages in stent graft modification time, and does not require 3D printing aortic model preoperatively, more appropriate for patients with critical condition who require emergency surgery.

Availability of Data and Materials

Datasets used and/or analyzed for this study are available from the corresponding author upon appropriate request.

Author Contributions

RZ and HY designed and gave the main idea of the research. RZ, QL, CC, WH, HZ, XH, HX conducted research and collected data, analyzed data, software operation and performed statistical measurements. RZ wrote the manuscript. FZ, KS contrasted collected data, analyzed data and critically examined the manuscript. All the authors have contributed to the editorial changes of the manuscripts. All the authors read and approved the final manuscript. All authors were fully involved in this work and agreed to take responsibility for all aspects of the work.

Ethics Approval and Consent to Participate

This study was approved by the Ethics Committee of Zhengzhou University Second Affiliated Hospital (Approval No: 2023167) and all patients signed informed consent before surgery.

Acknowledgment

Not applicable.

Funding

Funding sources: Scientific and Technological Project of the Education Department of Henan Province (232102310158). While the author has no financial and scientific relationship with the aortic covered stent company in the paper.

Conflict of Interest

The authors declare no conflict of interest.

References

- [1] MacGillivray TE, Gleason TG, Patel HJ, Aldea GS, Bavaria JE, Beaver TM, *et al.* The Society of Thoracic Surgeons/American Association for Thoracic Surgery clinical practice guidelines on the management of type B aortic dissection. *The Journal of Thoracic and Cardiovascular Surgery.* 2022; 163: 1231–1249.
- [2] Erbel R, Aboyans V, Boileau C, Bossone E, Bartolomeo RD, Eggebrecht H, *et al.* 2014 ESC Guidelines on the diagnosis and treatment of aortic diseases: Document covering acute and chronic aortic diseases of the thoracic and abdominal aorta of the adult. The Task Force for the Diagnosis and Treatment of Aortic Diseases of the European Society of Cardiology (ESC). *European Heart Journal.* 2014; 35: 2873–2926.
- [3] Huang Q, Chen XM, Yang H, Lin QN, Qin X. Effect of Left Subclavian Artery Revascularisation in Thoracic Endovascular Aortic Repair: a Systematic Review and Meta-analysis. *Journal of Vascular Surgery.* 2018; 68: 1959.
- [4] Chen X, Wang J, Premaratne S, Zhao J, Zhang WW. Meta-analysis of the outcomes of revascularization after intentional coverage of the left subclavian artery for thoracic endovascular aortic repair. *Journal of Vascular Surgery.* 2019; 70: 1330–1340.
- [5] Weigang E, Parker JA, Czerny M, Lonn L, Bonser RS, Carrel TP, *et al.* Should intentional endovascular stent-graft coverage of the left subclavian artery be preceded by prophylactic revascularisation? *European Journal of Cardio-Thoracic Surgery.* 2011; 40: 858–868.
- [6] Rimbau V, Böckler D, Brunkwall J, Cao P, Chiesa R, Coppi G, *et al.* Editor's Choice - Management of Descending Thoracic Aorta Diseases: Clinical Practice Guidelines of the European Society for Vascular Surgery (ESVS). *European Journal of Vascular and Endovascular Surgery.* 2017; 53: 4–52.
- [7] George MJ, Dias-Neto M, Ramos Tenorio E, Skibber MA, Morris JM, Oderich GS. 3D printing in aortic endovascular therapies. *The Journal of Cardiovascular Surgery.* 2022; 63: 597–605.
- [8] Ma L, Liu C, Guo XM, Pan YM, Zheng Z. The Application Value of 3D Printing in Individualized Endovascular Treatment of Complex Aortic Diseases. *Radiology Practice.* 2018; 33: 903–906. (In Chinese)
- [9] Ho D, Squelech A, Sun Z. Modelling of aortic aneurysm and aortic dissection through 3D printing. *Journal of Medical Radiation Sciences.* 2017; 64: 10–17.
- [10] Fu DS, Jin Y, Zhao ZH, Wang C, Shi YH, Zhou MJ, *et al.* Three-Dimensional Printing to Guide Fenestrated/Branched TEVAR in Triple Aortic Arch Branch Reconstruction with a Curative Effect Analysis. *Journal of Endovascular Therapy.* 2023. (online ahead of print)
- [11] Sun Z. 3D printing in medicine: current applications and future directions. *Quantitative Imaging in Medicine and Surgery.* 2018; 8: 1069–1077.
- [12] Marone EM, Auricchio F, Marconi S, Conti M, Rinaldi LF, Pietrabissa A, *et al.* Effectiveness of 3D printed models in the treatment of complex aortic diseases. *The Journal of Cardiovascular Surgery.* 2018; 59: 699–706.
- [13] Verghi E, Catanese V, Nenna A, Montelione N, Mastroianni C, Lusini M, *et al.* 3D Printing in Cardiovascular Disease: Current Applications and Future Perspectives. *Surgical Technology International.* 2021; 38: 314–324.
- [14] Chassin-Trubert L, Gandet T, Lounes Y, Ozdemir BA, Alric P, Canaud L. Double fenestrated physician-modified stent-grafts for total aortic arch repair in 50 patients. *Journal of Vascular Surgery.* 2021; 73: 1898–1905.e1.
- [15] Chassin-Trubert L, Mandelli M, Ozdemir BA, Alric P, Gandet T, Canaud L. Midterm Follow-up of Fenestrated and Scalloped Physician-Modified Endovascular Grafts for Zone 2 TEVAR. *Journal of Endovascular Therapy.* 2020; 27: 377–384.
- [16] Yuan D, Luo H, Yang H, Huang B, Zhu J, Zhao J. Precise treatment of aortic aneurysm by three-dimensional printing and simulation before endovascular intervention. *Scientific Reports.* 2017; 7: 795.
- [17] Liu CJ, Liu Z. 3D printing technology guided pre-opening window for the treatment of complex aortic arch lesions. *Chinese Journal of Practical Surgery.* 2018; 38: 1381–1384.
- [18] Liu Z, Li XR, Zhang M, Zhou MJ, Jiang Q, Zhou M, *et al.* 3D printing combined with stent bundle diameter technique for pre-

- triple fenestration in the treatment of Stanford type B aortic dissection in 1 case. *Chinese Journal of Vascular Surgery: Electronic Edition*. 2019; 11: 142–144. (In Chinese)
- [19] Tong Y, Qin Y, Yu T, Zhou M, Liu C, Liu C, *et al*. Three-Dimensional Printing to Guide the Application of Modified Prefenestrated Stent Grafts to Treat Aortic Arch Disease. *Annals of Vascular Surgery*. 2020; 66: 152–159.
- [20] Tong Y, Yu T, Zhou M, Liu C, Zhou M, Jiang Q, *et al*. Use of 3D Printing to Guide Creation of Fenestrations in Physician-Modified Stent-Grafts for Treatment of Thoracoabdominal Aortic Disease. *Journal of Endovascular Therapy*. 2020; 27: 385–393.
- [21] Akutsu K, Nejima J, Kiuchi K, Sasaki K, Ochi M, Tanaka K, *et al*. Effects of the patent false lumen on the long-term outcome of type B acute aortic dissection. *European Journal of Cardio-Thoracic Surgery*. 2004; 26: 359–366.
- [22] Trimarchi S, Tolenaar JL, Jonker FHW, Murray B, Tsai TT, Eagle KA, *et al*. Importance of false lumen thrombosis in type B aortic dissection prognosis. *The Journal of Thoracic and Cardiovascular Surgery*. 2013; 145: S208–S212.
- [23] Conrad MF, Crawford RS, Kwolek CJ, Brewster DC, Brady TJ, Cambria RP. Aortic remodeling after endovascular repair of acute complicated type B aortic dissection. *Journal of Vascular Surgery*. 2009; 50: 510–517.
- [24] Kang WC, Greenberg RK, Mastracci TM, Eagleton MJ, Hernandez AV, Pujara AC, *et al*. Endovascular repair of complicated chronic distal aortic dissections: Intermediate outcomes and complications. *The Journal of Thoracic and Cardiovascular Surgery*. 2011; 142: 1074–1083.
- [25] Gomes EN, Dias RR, Rocha BA, Santiago JAD, Dinato FJS, Saadi EK, *et al*. Use of 3D Printing in Preoperative Planning and Training for Aortic Endovascular Repair and Aortic Valve Disease. *Brazilian Journal of Cardiovascular Surgery*. 2018; 33: 490–495.
- [26] Hangge P, Pershad Y, Witting AA, Albadawi H, Oklu R. Three-dimensional (3D) printing and its applications for aortic diseases. *Cardiovascular Diagnosis and Therapy*. 2018; 8: S19–S25.
- [27] Spinelli D, Marconi S, Caruso R, Conti M, Benedetto F, Marrocc-Trischitta MM, *et al*. 3d Printed Aortic Models as a Teaching Tool for Trainees in Vascular Surgery. *European Journal of Vascular and Endovascular Surgery*. 2019; 58: e338–e339.
- [28] Sun Z, Squelch A. Patient-Specific 3D Printed Models of Aortic Aneurysm and Aortic Dissection. *Journal of Medical Imaging and Health Informatics*. 2017; 7: 886–889.
- [29] Wu C, Squelch A, Sun Z. Investigation of Three-dimensional Printing Materials for Printing Aorta Model Replicating Type B Aortic Dissection. *Current Medical Imaging*. 2021; 17: 843–849.